GEOPHYSICAL RESEARCH LETTERS, VOL. 28, NO. 15, PAGES 3015-3018, AUGUST 1, 2001

3-D crustal velocity structure at the rift tip in the western Woodlark Basin

Barry C. Zelt, Brian Taylor, and Andrew M. Goodliffe

School of Ocean and Earth Science and Technology, University of Hawaii, Honolulu, Hawaii, USA

Abstract. We present a three-dimensional (3-D) crustal velocity model for part of the western Woodlark Basin in the SW Pacific, where rifting of a continental arc transitions to seafloor spreading. Velocities to ~14 km depth are constrained by regularized inversion of first arrival traveltimes recorded at 14 ocean bottom instruments from a network of airgun profiles within an 80 km × 80 km area. The 3-D velocity model images the axis and flanks of the rift basin adjacent to the westernmost spreading segment. Velocity contours that dip north at ~10° parallel seismic reflectors from within a thick ophiolitic basement. High velocities (7.5 km/s) at the base of our model and preliminary analysis of earthquake P-wave arrival times are consistent with an average crustal thickness of 15–20 km. Anomalously shallow upper mantle (8 km/s) velocities occur 6 km south of the spreading center at a depth of 3 km below the seafloor, and in the western part of the model, ~30 km east of the D'Entrecasteaux Islands, at a depth of 6 km below the seafloor.

1. Introduction

The Woodlark Basin is a small ocean basin located between the easternmost Papuan Peninsula of New Guinea and the Solomon Islands in the southwest Pacific (Fig. 1 inset). Orogenically thickened crust of the Papuan Peninsula has been stretched and divided by westward propagation of seafloor spreading in the basin since at least 6 Ma [*Taylor et al.*, 1999a]. The western Woodlark Basin is one of the most seismically active continental rifts and has one of the highest extension rates (~3 cm/yr, ibid). Focal depths for teleseismically recorded earthquakes near the transition region between continental rifting and seafloor spreading are shallow (<10 km), and focal mechanisms for a number of these events permit normal slip on planes dipping at low-angles (25-35°; Fig. 1a) [*Abers*, 1991; *Abers et al.*, 1997]. Studies of other extensional systems have proposed that low-angle (<30°) normal faulting can accommodate large amounts of extensional strain; yet this hypothesis violates classical theories of frictional slip on faults which predict that normal faults in extensional provinces will form at high angles (~60°) [*Anderson*, 1942; *Buck*, 1988].

To investigate further the spreading/rifting dynamics in the transition area, and to help resolve the low-angle normal faulting paradox, an onshore/offshore seismic experiment was conducted in 1999-2000 in the western Woodlark Basin utilizing both passive and active sources. One of the primary objectives of this experiment is to accurately locate the microseismicity and determine if the earthquake hypocenters delineate a shallow dipping fault plane previously imaged by seismic reflection profiling [*Abers et al.*, 1997; *Mutter et al.*, 1996; *Taylor et al.*, 1995, 1999a]. To accomplish this requires an accurate 3-D velocity model. In this paper we present the results of a tomographic inversion for the 3-D velocity structure using first arrival traveltimes recorded on ocean bottom instruments from airgun blasts.

Paper number 2001GL012864.
0094-8276/01/2001GL012864$05.00

2. Study Region, Experiment and Data

The seismic study is centered on the easternmost area of rifting, adjacent the spreading tip (Fig. 1). *Goodliffe et al.* [1999] provide a summary of previous geophysical studies in the area that include the collection of complete bathymetry (Fig. 1a), acoustic imagery, magnetization, gravity and multi-channel seismic (MCS) data. A simplified N-S cross-section (Fig. 1b) shows the primary structures and stratigraphy inferred from seismic and drilling data. The active rift is an asymmetric graben bounded by a 27°±3° north-dipping fault and an antithetic fault dipping 45° south. Drilling into the footwall fault block (Moresby Seamount) as well as into the northern margin recovered dolerites and gabbro similar to the Paleocene-early Eocene island arc ophiolite that forms the regional basement [*Taylor et al.*, 1999b].

We deployed an array of 20 ocean bottom seismometers and hydrophones (OBS/Hs) over an area of 30 km × 30 km (Fig. 1a). Six instruments failed to return useful data. The remaining 14 instruments (7 OBSs and 7 OBHs) recorded microseismicity for up to 6 months beginning in September of 1999, but additionally at the beginning of the deployment recorded large (180 l) airgun blasts from a network of intersecting seismic profiles. We use first-arrival traveltimes from the airgun blasts to derive the 3-D crustal velocity structure. The shot interval was 100 s (~250 m) resulting in 3250 shots in the study region fired into the array. Shot locations, determined by GPS, are accurate to within 15 m. Water depths at the OBS/Hs are 2.1–3.2 km. OBS/H coordinates were determined by inverting approximately 150 water wave arrival times per instrument for location. Estimated instrument location errors range between 15 and 35 m. Because of battery failure, clock drift corrections of two instruments (Helmut and Salote; Fig. 1) were estimated based on expected traveltime differentials between various stations for teleseismic earthquakes recorded throughout the OBS/H deployment. We estimated no significant drift for OBS Helmut and 2.9±1.2 ms/day for OBS Salote. Shot-receiver offsets were limited to ~65 km. A total of 31,421 first arrival picks were made; uncertainties of 40-125 ms (average=70 ms) were assigned based on the signal-to-noise ratio of the data in the vicinity of the pick. Figure 1c shows the data from shot

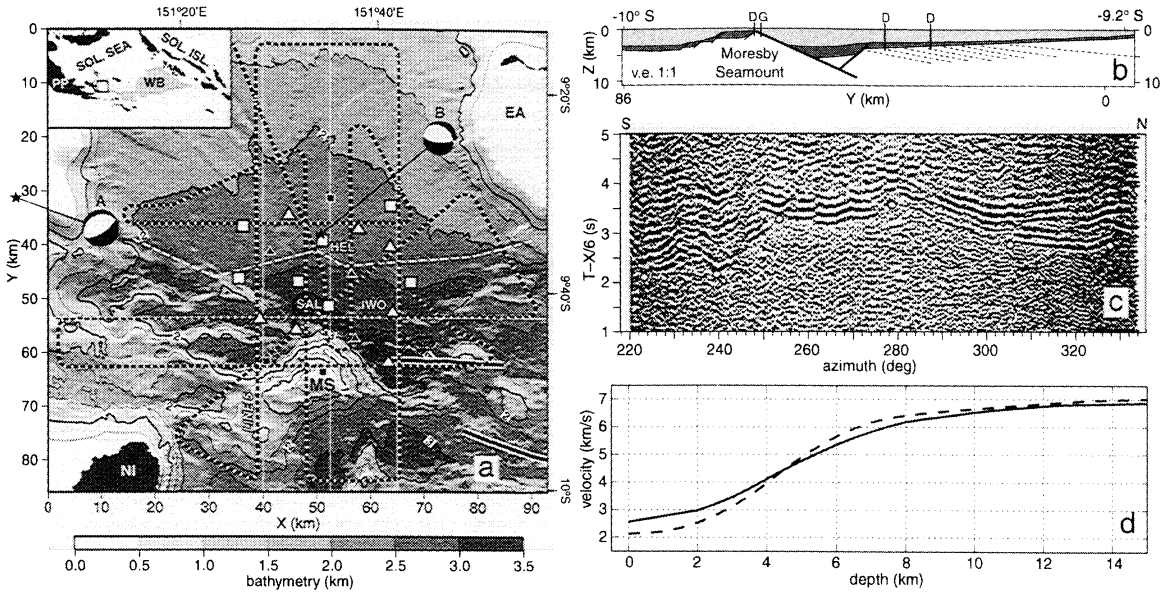

Figure 1. (a) Experiment geometry and bathymetry in the western Woodlark Basin. Squares/triangles are OBS/Hs. Smaller black symbols are instruments that failed. Named instruments mentioned in text are HEL=Helmut, IWO=Iwo Jima, SAL=Salote. Black and white broken line is the ship track (shot point locations). Focal mechanisms for two earthquakes (stars) consistent with shallow-dipping normal faulting are shown. Solid, white-outlined black lines in the SE are the axes of the two western-most spreading centers. Broken white line is the northern limit of the rift basin. Region to the north is the Woodlark Rise. Thin white lines are the locations of vertical slices in Fig. 2 d and e. EA, Egum Atoll; MS, Moresby Seamount; NI, Normanby Island. Bathymetry contour interval is 0.5 km. Inset map shows location of study area (square) in relation to oceanic crust (gray) of the Woodlark Basin (WB), Papuan Peninsula (PP), Solomon Sea (Sol. Sea), and Solomon Islands (Sol. Isl.). (b) Simplified interpretation of seismic reflection data along x=52.5 km showing Moresby Seamount and the fault-bounded rift basin to the north [after *Taylor et al.*, 1995]. Dip angles of south- and north-dipping faults are approximately 27° and 45°, respectively. Light gray is water. Dark gray is Miocene-Pleistocene sediments. Shallow (≤11°) north-dipping lines within basement represent predominant fabric observed in MCS data [*Goodliffe et al.*, 1999]. Vertical lines are drill sites labeled according to basement rock type: D, dolerite; G, gabbro. Vertical exaggeration is 1:1. (c) Record section from shot line 5 recorded at OBH Iwo Jima. Offset range of data is 25–55 km. Data are reduced at 6 km/s and bandpass filtered between 3–13 Hz. Horizontal scale is receiver to shot azimuth measured clockwise from north. Dots show first arrival picks at various locations. (d) 1-D starting velocity model (broken line) and average 1-D velocity structure of the final 3-D model (solid line).

line 5 recorded at OBH Iwo Jima. First arrivals on this section can be observed to offsets of 50 km. The relatively early first arrival times in the south echo the shallow bathymetry southwest of the Moresby Seamount.

3. Method

Our objective was to derive the smoothest model overall which provides a normalized χ^2 misfit to the data of 1. To derive the 3-D velocity structure we used the first-arrival traveltime tomography method of *Zelt and Barton* [1998], with modifications to minimize the size and roughness of the perturbation from a background model. This method is iterative and requires a starting model; new ray paths are calculated for each iteration. For the forward step, traveltimes are calculated on a uniform (0.5 km node spacing) 3-D velocity grid using a finite-difference solution to the eikonal equation [*Vidale* 1990], with modifications to handle large velocity gradients and contrasts [*Hole and Zelt* 1995]. A cell size of 2×2×0.5 km was used for the slowness grid in the inverse step. Model dimensions are 94×86×15.5 km. Unless otherwise specified, depths mentioned in this paper are relative to sea level.

The modeling and resolution analysis follows very closely the procedure described in *Zelt et al.* [2001], and thus for brevity we outline only the key steps. A 1-D (laterally homogenous) starting model (Fig. 1d) was derived by trial and error forward modeling of the average first-arrival traveltimes versus offset for the entire dataset. The water layer was effectively stripped off by moving the shots to the seafloor. The root-mean-square (RMS) misfit for the 1-D starting model was 354 ms (χ^2=40). To quantitatively assess the resolution of the data, we performed checkerboard resolution tests and used the results of these tests to generate maps of estimated lateral resolution at each point of the model using the method described in *Zelt* [1998].

4. Results

The final model was obtained after 11 iterations and provides a RMS data misfit of 63 ms (χ^2=1). The available shot-receiver offsets restricted the maximum depth of ray penetration to about 14 km. Horizontal and vertical slices through the final model are shown in Fig. 2a, d and e. The results of a checkerboard resolution test (Fig. 2b) show that to a depth of 10 km lateral velocity variations in the order of 10

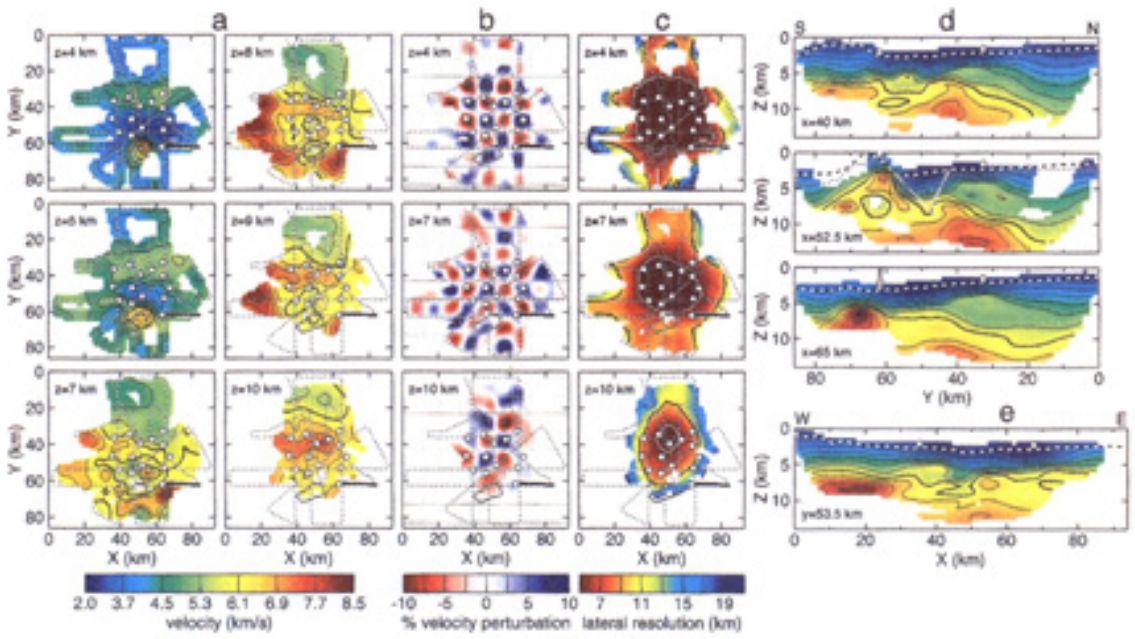

Figure 2. 3-D model and results of resolution tests. (a) Horizontal slices through the final model at the depths indicated. Circles are OBS/Hs. Black and white broken line denotes shot point locations. Short, thick black line in the SE is the western-most rift axis. Thick gray line is the 1-km bathymetric contour of the Moresby Seamount. Contour interval is 0.5 km/s. Heavy black line is the 6 km/s contour. Note that the velocity scale is not linear. Regions not sampled by ray paths are white. (b) Results of a checkerboard test showing horizontal slices of relative velocity perturbations with respect to the starting model for a checkerboard cell size of 10 km and true perturbation of ±10% from the starting model. Gray lines outline the checkerboard grid. (c) Horizontal slices of estimated lateral velocity resolution using the method of *Zelt* [1998]. Contour interval is 5 km. Heavy black line is the 10 km contour. White line is the 5 km contour. (d) Vertical slices parallel to the y-axis. Velocity scale and contours are same as panel (a). Vertical exaggeration is 2:1. Heavy dashed line is the bathymetry at the location of the slice. Two circles along top represent range of model covered by OBS/H receivers. On x=52.5 km slice: gray lines show shallow S-dipping, and steeper antithetic N-dipping faults discussed in text; thin dotted line is base of sediments (based on MCS images). Arrow on the x=65 km slice marks the location of the rift axis. (e) Same as d but for a slice parallel to the x-axis at y=53.5 km.

km are generally well-resolved. A suite of checkerboard resolution tests was used to derive a map of lateral velocity resolution (Fig. 2c) [*Zelt*, 1998]; resolution is highest (generally better than 10 km) in the vicinity of the OBS/H array.

The velocity structure is, with a number of exceptions, broadly two-dimensional, trending east-west. North of Moresby Seamount, an east-west band of shallow low velocities represent rift basin sediments. The tomographic model depicts the sharp rift basin boundaries seen in the MCS data (Fig. 1b) as velocity gradients. Nevertheless, in the corresponding vertical cross-section at x=52.5 km (Fig. 2d), the model clearly delineates the boundary between the high-velocity seamount fault block and the rift basin sediments at depths <5 km. Further north (y≤40 km), isovelocity contours dip consistently northward (~10°), as do strong intra-basement reflectors observed in MCS data [*Goodliffe et al.*, 1999]. In the northwest (x=40 km, Fig. 2d), there is a thick (5-7 km at y=10 km) Miocene forearc basin [*Fang*, 2000]. Near-upper mantle velocities (7-7.5 km/s) are reached at depths of 10-14 km within a narrow east-west zone along y≈40 km. The shot data do not provide ray coverage below 14 km but we can estimate crustal thickness from seismicity recorded at the ocean bottom array. Preliminary analysis shows that the crossover point from crustal to upper mantle velocities for P-wave arrival times occurs at 80–100 km indicating an average crustal thickness of 15–20 km in the area of Fig. 1a. This crustal thickness estimate is similar to that of the intra-oceanic Izu-Bonin island arc [*Suyehiro et al.*, 1996] that has been interpreted as an in situ ophiolite [*Bloomer et al.*, 1995]. In contrast to this and oceanic crust, however, relatively low velocity (<6 km/s) rocks comprise a far greater fraction of Woodlark Rise crust. Given that mafic rocks with lab velocities of 6 km/s have been drilled in four locations within the ophiolitic basement of the study area [*Taylor et al.*, 1999], we infer that fracture porosity is responsible for the velocity reduction.

Three anomolously high velocity features disrupt the general 2-D trend: (1) the Moresby Seamount down to depths of 5 km; (2) south of the western-most spreading tip at depths ≥6 km; and (3) west of x=30 km at depths ≥8 km. The high velocities beneath the Moresby Seamount are consistent with the gabbroic basement drilled there (Fig. 1b). The high-velocity anomaly ~6 km south of the rift tip (x=65 km; Fig. 2d) may demark a substantial thinning of the crust with upper mantle (8 km/s) velocities occurring only 3 km below the seafloor. If this feature is genetically related to seafloor spreading, it is offset significantly from the rift axis; synthetic modeling shows that the off-axis position of the anomaly is not an artifact of the experiment geometry. Most enigmatic are the high (>8 km/s) velocities at depths of 8 km to the west of the OBS/H array (z=8, 9 km and y=53.5 km; Fig. 2a and e).

If the high velocities represent upper mantle, crustal thickness here is only 6 km. Unfortunately we have no ray coverage below 9 km in this region of the model (Fig. 2e) and so cannot determine if the 8 km/s material extends deeper, or whether we are imaging an anomalous high-velocity crustal layer. Integration of our findings with results from regional studies using the land based seismic arrays [e.g., *Ferris et al., 2000; Floyd et al.,* 2000] will allow us to resolve the nature of the velocity anomalies.

5. Conclusions

We have derived a 3-D crustal velocity model for the easternmost rift segment adjacent the spreading tip of the western Woodlark Basin. The velocity model images the rift basin, the southern footwall fault block (Moresby Seamount), and ~10°-north-dipping ophiolitic crust to the north. Anomolously-shallow upper mantle-type velocities occur in the western part of our study area and south of the western-most spreading center. Apart from these anomalies, upper mantle velocities are not reached in the model, but high (7–7.5 km/s) velocities near the center of our model and arrival times from regional seismicity are consistent with a crustal thickness of 15–20 km. Basement velocities are generally lower than expected for normal oceanic crust or in comparison to intra-oceanic (ophiolitic) island arc crust. The velocity model will be essential for locating the microseismicity recorded during the 6-month OBS/H deployment in this active rift.

Acknowledgments. These results form part of an NSF-sponsored investigation of seismicity in PNG with J. Mutter, B. Taylor, G. Abers and A. Lerner-Lam as co-PIs, and M. Craig, H. Davies and S. Sioni as PNG collaborators. Special thanks to the Scripps and Lamont OBS/H teams (Jeff Babcock, Paul Zimmer, Ted Koczynski and Russell Johnson), and to the scientists and crew of R/V Ewing cruises 9910 and 0002, for deploying and recovering the instruments.

References

Anderson, D.M., The Dynamics of Faulting, 183 pp, Oliver and Boyd, Edinburgh, 1942.

Abers, G.A., Possible seismogenic shallow-dipping normal faults in the Woodlark-D'Entrecasteaux extensional province, Papua New Guinea, *Geology, 19*, 1205-1208, 1991.

Abers, G.A., C.Z. Mutter, and J. Fang, Shallow dips of normal faults during rapid extension: Earthquakes in the Woodlark-D'Entrecasteaux rift system, Papua New Guinea, *J. Geophys. Res., 102*, 15,301–15,317, 1997.

Bloomer, S.H., B. Taylor, C.J. MacLeod, R.J. Stern, P. Fryer, J.W. Hawkins, and L. Johnson, Early arc volcanism and the ophiolite problem: a perspective from drilling in the western Pacific, in *Active Margins and Marginal Basins of the Western Pacific*, edited by B. Taylor, and J. Natland, *Geophysical Monograph 88, AGU*, 1–30, 1995.

Buck, W.R., Flexural rotation of normal faults, *Tectonics, 7*, 959-973, 1988.

Fang, J., Styles and distribution of continental extension derived from the rift basins of eastern Papua New Guinea, [Ph.D. thesis] Columbia University, New York, 2000.

Ferris, A., G.A. Abers, J. Floyd, A. Lerner-Lam, J. Mutter, M. Craig, H. Davies, S. Sioni, and B. Taylor, Active continental extension and metamorphic core complexes: a PASSCAL seismic deployment in the D'Entrecasteaux Islands, eastern Papua New Guinea, *EOS Trans. AGU, 81*, F881, 2000.

Floyd, J.S., J. Mutter, A. Lerner-Lam, W. Menke, G.A. Abers, A. Ferris, B. Taylor, B.C, Zelt, M. Craig, H. Davies, and S. Sioni, Rapid changes in crustal thickness associated with mid-ocean ridge propagation into continental lithosphere in the western Woodlark Basin, *EOS Trans. AGU, 81*, F115, 2000.

Goodliffe, A.M., B. Taylor, and F. Martinez, Data report: Marine Geophysical surveys of the Woodlark Basin region, in Proc. ODP, Init. Repts, edited by B. Taylor, P. Huchon, A. Klaus, et al., 180, 1-120 [CD-ROM], 1999, Ocean Drilling Program, Texas A&M University, College Station, Texas.

Hole, J.A., and B.C. Zelt, Three-dimensional finite-difference reflection travel times, *Geophys. J. Int., 121*, 427-434, 1995.

Mutter, J.C., C.Z. Mutter, and J. Fang, Analogies to oceanic behaviour in the continental breakup of the western Woodlark basin, *Nature, 380*, 333–336, 1996.

Suyehiro, K., N. Takahashi, Y. Ariie, Y. Yokoi, R. Hino, M. Shinohara, T. Kanazawa, N. Hirata, H. Tokuyama, A. Taira, Continental crust, crustal underplating, and low-Q upper mantle beneath an oceanic island arc, *Science, 272*, 390–392, 1996.

Taylor, B., A. Goodliffe, F. Martinez, R. Hey, Continental rifting and initial sea-floor spreading in the Woodlark basin, *Nature, 374*, 534–537, 1995.

Taylor, B., A.M. Goodliffe, and F. Martinez, How continents break up: Insights from Papua New Guinea, *J. Geophys. Res., 104*, 7497-7512, 1999a.

Taylor, B., Background and regional setting for ODP Leg 180, in Proc. ODP, Init. Repts, edited by B. Taylor, P. Huchon, A. Klaus, et al., 180, 1-120 [CD-ROM], 1999b, available from: Ocean Drilling Program, Texas A&M University, College Station, Texas.

Vidale, J.E., Finite-difference calculation of travel times in three dimensions, *Geophysics, 55*, 521-526, 1990.

Zelt, B.C., R.M. Ellis, C.A. Zelt, R.D. Hyndman, C. Lowe, G.D. Spence, and M.A. Fisher, Three-dimensional crustal velocity structure beneath the Strait of Georgia, British Columbia. *Geophys. J. Int., 144*, 695–712, 2001.

Zelt, C.A., Lateral velocity resolution from three-dimensional seismic refraction data, *Geophys. J. Int., 135*, 1101-1112, 1998.

Zelt, C.A., and P.J. Barton, 3D seismic refraction tomography: A comparison of two methods applied to data from the Faeroe Basin, *J. Geophys. Res., 103*, 7187-7210, 1998.

B.C. Zelt, B. Taylor, and A.M. Goodliffe, School of Ocean and Earth Science and Technology, University of Hawaii, 1680 East-West Road, Honolulu, HI 96822. (bzelt@soest.hawaii.edu; taylor@soest.hawaii.edu; andrew@soest.hawaii.edu)

(Received January 10, 2001; revised May 3, 2001;
accepted May 18, 2001)